Ground State of 1,6-Bridged [10] Annulenes: Infrared and Raman Spectra and Density Functional Calculations

Cristina Gellini and Pier Remigio Salvi*

Laboratorio di Spettroscopia Molecolare, Dipartimento di Chimica, Universitá di Firenze, via Gino Capponi 9, 50121 Firenze, Italy

Emanuel Vogel

Institut für Organische Chemie, Universität zu Köln, Greinstrasse 4, 50939 Köln, Germany

Received: October 29, 1999; In Final Form: January 11, 2000

The infrared and Raman spectra of 1,6-methano[10]annulene and 1,6-epoxy[10]annulene, higher homologues of benzene with 10 π electrons, have been measured at room temperature in solution and in the solid phase. Density functional calculations using the B3-LYP functional and the 6-31G** basis set have been performed on the aforementioned molecules, on the 11,11-dicyano and 11,11-dimethyl derivatives of 1,6-methano[10]-annulene, and on naphthalene. In general, the calculated molecular structures are in good agreement with X-ray data. The calculation of the vibrational frequencies and intensities of 1,6-methano[10]annulene and 1,6-epoxy[10]annulene allows a complete assignment of their spectrum in terms of bridge and ring modes. A correlation is attempted with the modes of naphthalene.

I. Introduction

According to Hückel MO theory, [10]annulenes possessing a planar (or near planar) ring skeleton are supposed to represent the next higher aromatic homologues of benzene.[1,2] However, all-*cis*- and mono-*trans*-[10]annulene, the two known simple [10]annulenes, do not meet the steric criterion for aromaticity, since they exist in pronouncedly nonplanar conformations.[3] As a consequence, both of these molecules are highly reactive polyolefins. Di-*trans*-[10]annulene which, due to the presence of two sterically interfering inside hydrogen atoms, starkly deviates from planarity has never yielded to synthesis.

In line with theory, 1,6-methano-, 1,6-epoxy-, and 1,6-imino-[10]annulene (**1**, **2**, and **3** of Figure1, respectively), in which the 10-membered ring has been forced into an approximately planar conformation by replacement of 1,6-positioned hydrogen atoms by CH_2, O, or NH groups, are found to be aromatic.[4−10] Similarly, 1,5-methano[10]annulene and the totally planar 1,6-didehydro[10]annulene, derived from [10]annulene by introduction of acetylene−cumulene bonds,[11] constitute "Hückel aromatics".

It is a special feature of 1,6-bridged [10]annulenes that they may be in rapid equilibrium with norcaradiene-type tautomers. While the parent hydrocarbon is present as the aromatic [10]-annulene **1**,[12] its derivatives in which the two bridge hydrogen atoms have been substituted by π acceptor groups predominantly or exclusively exist as norcaradienic tautomers (structure **5** of Figure 2).[13−15] Interestingly, apart from aromatic also olefinic 1,6-methano[10]annulenes are known (structure **4** of Figure 2). A case in point is 2,5,7,10-tetra(trimethylsilyl)-1,6-methano-[10]annulene, where the bulky substituents next to the bridge bring about distortion of the 10-membered ring leading to a [10]annulene with fluctuating π bonds.[16] Structural information on 1,6-epoxy[10]annulene (**2**) is scarce.[17]

* To whom correspondence should be addressed. E-mail: salvi@chim.unifi.it.

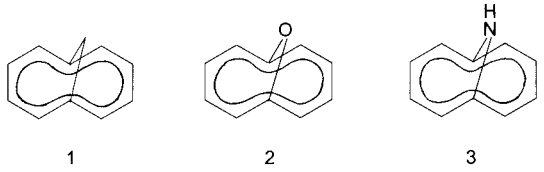

Figure 1. Molecular structures of 1,6-methano- (**1**), 1,6-epoxy- (**2**), and 1,6-imino[10]annulene (**3**).

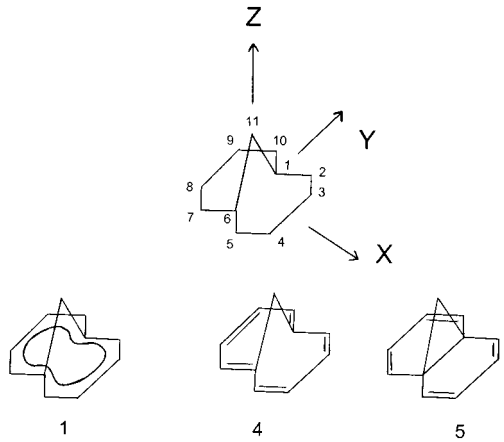

Figure 2. (top) Atomic numbering of bridged[10]annulenes and molecular reference system. (bottom) Structures of bridged[10]annulenes: **1**, aromatic; **4**, polyolefinic; **5**, norcaradienic.

1,6-Bridged[10]annulenes, specifically **1** and **2**, stand out among the diverse types of [10]annulenes hitherto described in that they can be synthesized on preparative scale and, moreover, are stable compounds.[18] Over the years, this type of [10]-annulenes has thus been subject to intense structural,[12−15] spectroscopic,[19−24] and chemical[18] scrutiny. Strange to say, however, detailed investigations of the vibrational spectra of these molecules have as yet not been forthcoming. In view of

10.1021/jp993849e CCC: $19.00
Published on Web 03/17/2000

the valuable information vibrational properties may provide, we have initiated a research program aimed at the analysis of the infrared and Raman spectra of [4*n* + 2]annulenes (*n* ≥ 2), starting with **1** and **2**, according to normal mode calculations based on the density functional (DF) approach. A related study has been recently performed on tetraazaannulenes.[25] The present study is intended to characterize the molecular force field of such annulenes in terms of vibrational frequencies and intensities. The vibrational analysis is made easier in the solid phase where only one conformation is usually present while it may become difficult in solution if a tautomeric equilibrium occurs.

II. Experimental Section

The synthesis of **1** and **2** has been described elsewhere.[4,18] The purity of both samples was checked by gas chromatographic analysis. Despite their chemical stability, the compounds were stored at −10 °C in the dark.

Solutions 10^{-1} M of **1** and **2** in CS_2 and CCl_4 were prepared for infrared measurements at room temperature. Infrared spectra of thin polycrystalline films were taken at room temperature by melting the material (**1**, mp 302 K; **2**, mp 325 K) between two KBr windows (3500−400 cm^{-1}) or two CsI windows to extend the spectral range of investigation to ≈200 cm^{-1}. The infrared spectra were measured on a FTIR interferometer (Bruker Model IFS 120 HR) with medium resolution conditions, ≈2 cm^{-1}.

The Raman spectra were measured in the range of 150−1700 cm^{-1} on a micro Raman instrument consisting of a Jobin-Yvon double monochromator coupled with an Olympus BH2 microscope and 100× objective for simultaneous excitation and collection. A notch filter was inserted along the optical collection system for stray light rejection. The Kr^+ laser line at 647.1 nm with typical power ≤1 mW at the sample was used for excitation. The detection system is a liquid nitrogen cooled CCD (charge coupled device) with an integration time of 300 s per spectral portion (≈500 cm^{-1}). These spectra were normalized each to the other using conventional software. The Raman spectra were also measured between 20 and 3500 cm^{-1} with standard instrumentation (Ar^+ laser, 514.5 nm; double monochromator, $\Delta\nu \approx 2$ cm^{-1}; red-extended cooled photomultiplier), placing the polycrystalline sample on the hollow tip of an holder and mildly focusing the excitation beam on the sample. With a laser power of 30 mW no sample damage was noticed and the spectra did not show change with the irradiation time. The intensities of the Raman lines were found substantially constant with the excitation wavelength.

The infrared and Raman measurements were performed also on naphthalene (Carlo Erba) under the same experimental conditions.

III. Results

A. MO ab Initio Calculations. In the past years several calculations have been made on the ground state of 1,6-methano-[10]annulene.[24,26−32] Three different extrema were found in the RHF approximation, corresponding to structures **1**, **4**, **5** of Figure 2.[24,30] Two of them, i.e., **4** and **5**, are local minima while **1** is a saddle point on the S_0 energy surface.[24] Correlation effects, taken into account with MP2 corrections to RHF results, reverse the energy ordering and favor the aromatic structure **1**. Further, DF calculations show that structures **4** and **5** converge to **1** through optimization and therefore that **1** is the only minimum on S_0.[24]

For the purpose of the present paper, additional DF calculations using the B3-LYP exchange-correlation functional[33,34] and an extended basis set, 6-31G**, have been performed on 1,6-methano[10]annulene, its 11,11-dicyano and 11,11-dimethyl derivatives, 1,6-epoxy[10]annulene, and naphthalene with the GAUSSIAN 98 suite of programs.[85] As to the bridged unsubstituted [10]annulenes, only one stable, i.e., corresponding to all real vibrational frequencies, C_{2v} geometry is found. In particular, all of the C atoms of **2**, except C_1 and C_6 (see Figure 2 for numbering) belong to the same plane, as observed experimentally,[17] and the distances of the C_1 (or C_6) and the oxygen atoms from this plane are 0.36 and 1.21 Å, respectively (0.35 and 1.25 Å, experimental values). In contrast with **2**, the C_2, C_5 and C_3, C_4 atom pairs of **1** are calculated at different *z* coordinates and the molecule appears slightly bent downward along *z*, in agreement with X-ray data.[12] The C−C bond lengths of **2** are almost constant and close to the reported 1.39 Å value.[17] The relevant structural parameters of **1**, **2**, and naphthalene[36] are collected in Table 1.

TABLE 1: Experimental and Calculated (DF/B3-LYP Results, 6-31G Basis Set) Distances (Å) of Naphthalene (NA), 1,6-Methano[10]annulene (1) and 1,6-Epoxy[10]annulene (2)[a]**

	NA		**1**		**2**[b]	
	expt[c]	calcd	expt[d]	calcd	expt[e]	calcd
C_1-C_2	1.425	1.421	1.402	1.410	1.39	1.400
C_2-C_3	1.377	1.376	1.378	1.393	1.39	1.396
C_3-C_4	1.417	1.417	1.417	1.426	1.39	1.416
C_1-C_{11}			1.484	1.493		
C_1-O					1.43	1.392
$C_1\cdots C_6$	1.424	1.434	2.235	2.284	2.22	2.214

[a] Atom pairs in the first column are numbered as in Figure 2. [b] The calculated distances of C_1, or C_6, and of the oxygen atom from the plane defined by the eight ring carbon atoms, 2, 3, 4, 5 and 7, 8, 9, 10 in Figure 2, are 0.36 and 1.21 Å (0.35 and 1.25 Å, experiment), respectively. [c] From ref 33. [d] From ref 11. [e] From ref 15.

TABLE 2: Experimental and Calculated (DF/B3-LYP Results, 6-31G Basis Set) Distances (Å) of 1,6-Methano[10]annulene (1) and its 11,11-Dicyano (CNMA) and 11,11-Dimethyl (MeMA) Derivatives[a]**

	1		CNMA			MeMA	
	expt[b]	calcd	expt[c]	calcd[d]	calcd[e]	expt[f]	calcd
C_1-C_2	1.402	1.410	1.474	1.478	1.413	1.459	1.426
C_2-C_3	1.378	1.393	1.334	1.348	1.386	1.357	1.382
C_3-C_4	1.417	1.426	1.439	1.455	1.425	1.432	1.427
C_1-C_{11}	1.484	1.493	1.566	1.580	1.521	1.510	1.515
$C_1\cdots C_6$	2.235	2.284	1.542	1.558	2.253	1.827	2.167

[a] Atom pairs in the first column are numbered as in Figure 2. [b] From ref 11. [c] From ref 14. [d] Calculated type **5** or "norcaradienic" minimum of CNMA, $E = -609.5843$ hartrees. [e] Calculated type **1** or "aromatic" minimum of CNMA, $E = -609.5849$ hartrees. [f] From ref 12.

It is however known that bond-equalized structures such as **1** are preferred at the correlation level of theory.[37−39] DF calculations have been therefore performed on the 11,11-dicyano and 11,11-dimethyl derivatives whose molecular structures, as derived from X-ray diffraction data on the crystals[13,15] are of norcaradienic type **5**. It may be seen from Table 2 that the DF calculation predicts correctly the norcaradienic minimum (all associated frequencies being real) of the dicyano system with C_1-C_6 distance 1.542 Å (experimental value 1.558 Å). A second **1**-type minimum, almost degenerate with the norcaradienic **5**, is also found from the calculations. Only one minimum is calculated for the 11,11-dimethyl derivative. The ring C−C distances are in fair agreement with experiment.[13] However, the transannular length $C_1\cdots C_6$, 2.167 Å, differs largely from the observed value, 1.827 Å.[13] According to calculations, the

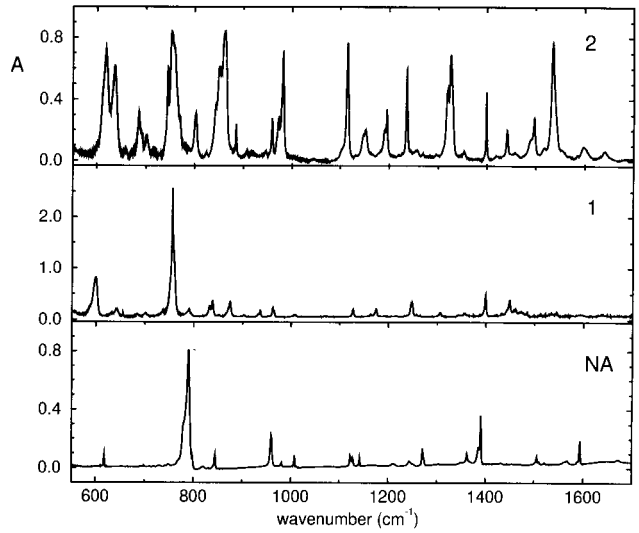

Figure 3. Infrared spectra of naphthalene (lower, NA), 1,6-methano-[10]annulene (middle, **1**), and 1,6-epoxy[10]annulene (upper, **2**) as polycrystalline films between KBr windows at room temperature in the range 600−1700 cm^{-1}.

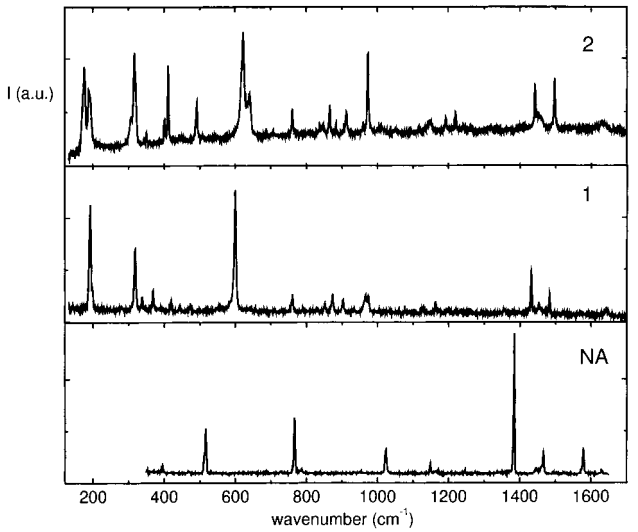

Figure 4. Raman spectra of polycrystalline naphthalene (lower, NA), 1,6-methano[10]annulene (middle, **1**), and 1,6-epoxy[10]annulene (upper, **2**) at room temperature in the range 150−1700 cm^{-1}. The relative intensities of the three spectra are normalized to the respective strongest peaks.

molecule is more similar to a strongly perturbed aromatic than to a norcaradienic system.

B. The Vibrational Spectra of Bridged [10]Annulenes. Under C_{2v} symmetry (with x and y the through-bond and through-atom axes, respectively; see Figure 2) the vibrational modes of **1**, 57, are classified into $16A_1$, $13A_2$, $14B_1$, and $14B_2$, and those of **2**, 51, into $14A_1$, $12A_2$, $12B_1$, and $13B_2$. Assuming the interaction between ring and bridge internal coordinates to be small, three modes of **2** may be approximately classified as hindered oxygen translations ($A_1 + B_1 + B_2$), six of **1** as hindered CH_2 translations and rotations ($A_1 + A_2 + 2B_1 + 2B_2$), and three of **1** as localized CH_2 modes of bending (A_1) and stretching (A_1, B_1) character. In this approximation the remaining, $13A_1$, $12A_2$, $11B_1$, and $12B_2$, are ring modes. For the sake of simplicity our vibrational analysis does not consider the eight C−H stretchings of the ring ($2A_1$, $2A_2$, $2B_1$, and $2B_2$).

The infrared and Raman spectra of polycrystalline naphthalene, 1,6-methano[10]annulene, and 1,6-epoxy[10]annulene are reported in Figures 3 and 4, respectively, naphthalene representing the system unaffected by the structural distortion. On inspection, the similarity of the infrared spectra of naphthalene and 1,6-methano[10]annulene is apparent. Due to symmetry lowering, the spectrum of **1** shows a larger number of bands than naphthalene. Both spectra are dominated by a single band, 790 cm^{-1} in naphthalene and 755 cm^{-1} in **1**. The infrared solution spectra of **1** and **2** (see Figures 6 and 8) have a similar spectral pattern, the band around 750 cm^{-1} being in both cases much stronger than all the others. In contrast with **1**, most infrared bands of the epoxy system **2** in the crystal phase are of comparable strength. The Raman spectra of the two bridged annulenes show intense peaks in the low energy region, $\nu \leq$ 700 cm^{-1}. The lines at 193, 318, and 600 cm^{-1} (**1**) and 176, 189, 318, 411, and 623 cm^{-1} (**2**) are the strongest. The same modes of **1** are active also in the fluorescence spectrum at low temperature.[24]

The vibrational assignment is based on DF/B3-LYP calculations (6-31G** basis set) of vibrational frequencies and infrared and Raman intensities. The harmonic frequencies have been scaled by an uniform factor, which corrects for the anharmonicity of the molecular vibrations. Since no scaling factor is reported for the DF/B3-LYP (6-31G**) combination,[40,41] a calculation was performed on naphthalene, with the purpose of determining the appropriate factor and transferring it to the bridged annulenes. It turns out that the vibrational frequencies of naphthalene are multiplied, on the average, by 0.989 below 1000 cm^{-1} and by 0.972 above 1000 cm^{-1} for best fit to experiment. For simplicity a single scaling factor, 0.979, has been assumed. This makes the scaled C−C frequencies slightly overestimated. Despite this, an overall excellent agreement with the observed spectra of naphthalene is found, as shown in Figure 5. The factor has therefore been considered to be sufficiently reliable for use also in the vibrational calculations of **1** and **2**.

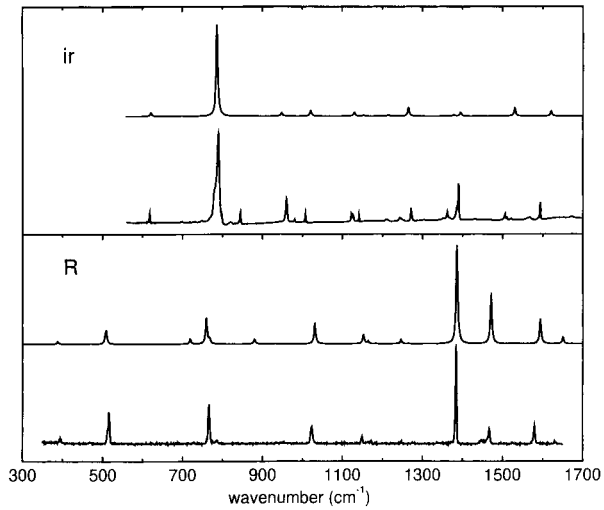

Figure 5. Experimental and calculated (DF/B3-LYP, 6-31G** basis set) vibrational spectra of naphthalene. Lower: Raman (R) spectrum. Upper: infrared (ir) spectrum. Calculated spectra, Lorentzian full band width, 2Γ, equal to 5 cm^{-1}. Relative intensities on the vertical axis are scaled to make the strongest peaks match in appearance.

Crystal field effects may affect the spectra. **1** and **2** crystallize in the orthorhombic system, space group $Fdd2(C_{2v}^{19})$ and $Pbca$-(D_{2h}^{15}), respectively, with four and eight molecules in the primitive unit cell located on C_1 sites.[12,17] As a result, each vibration of **2** is split into eight components (A_g, B_{1g}, B_{2g}, B_{3g}, A_u, B_{1u}, B_{2u}, B_{3u}), the "g" members of the multiplet being Raman while the "u" (except A_u) being infrared active. No coincidence between infrared and Raman bands is expected. In

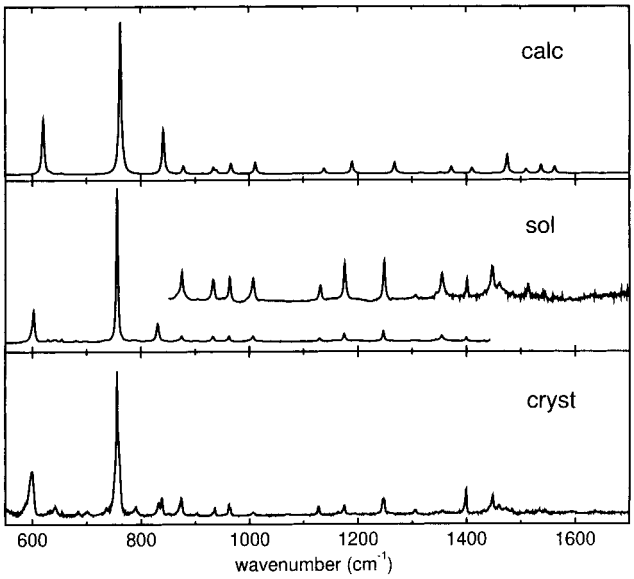

Figure 6. Experimental and calculated (DF/B3-LYP, 6-31G** basis set) infrared spectra of 1,6-methano[10]annulene. Lower: polycrystalline film (cryst) between KBr windows. Middle: solution (sol), 10^{-1} M in CS_2 (600−1300 cm^{-1}) and CCl_4 (800−1700 cm^{-1}). Upper: calculated spectrum (calc), Lorentzian full band width, 2Γ, equal to 5 cm^{-1}. Relative intensities on the vertical axis are scaled to make the strongest peaks match in appearance.

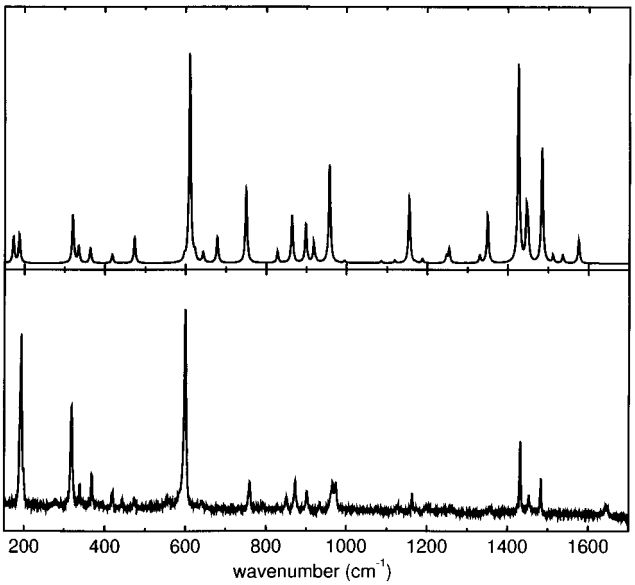

Figure 7. Experimental and calculated (DF/B3-LYP, 6-31G** basis set) Raman spectra of 1,6-methano[10]annulene. Lower: polycrystalline sample. Upper: calculated spectrum, Lorentzian full band width, 2Γ, equal to 5 cm^{-1}. Relative intensities on the vertical axis are scaled to make the strongest peaks match in appearance.

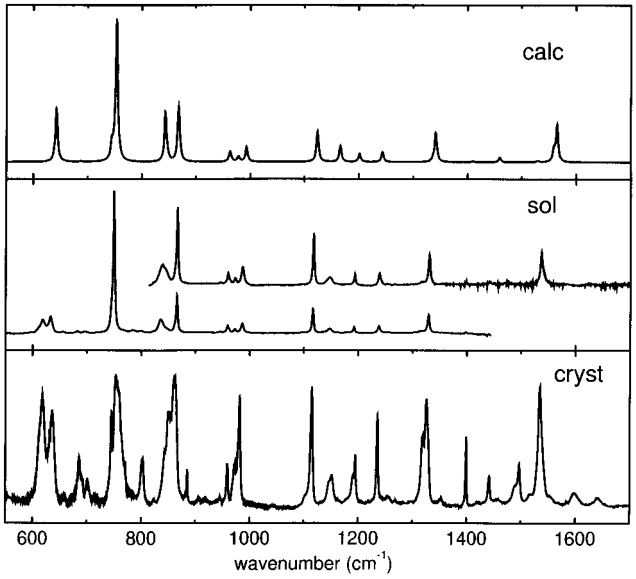

Figure 8. Experimental and calculated (DF/B3-LYP, 6-31G** basis set) infrared spectra of 1,6-epoxy[10]annulene. Lower: polycrystalline film (cryst) between KBr windows. Middle: solution (sol), 10^{-1} M in CS_2 (600−1300 cm^{-1}) and CCl_4 (800−1700 cm^{-1}). Upper: calculated spectrum (calc), Lorentzian full band width, 2Γ, equal to 5 cm^{-1}. Relative intensities on the vertical axis are scaled to make the strongest peaks match in appearance.

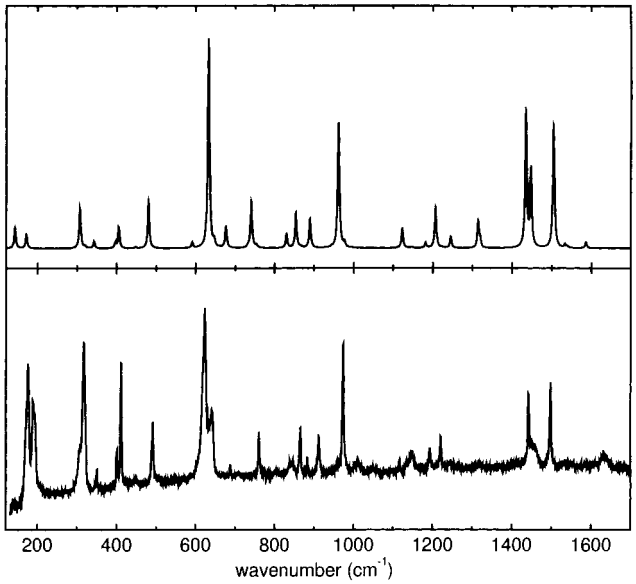

Figure 9. Experimental and calculated (DF/B3-LYP, 6-31G** basis set) Raman spectra of 1,6-epoxy[10]annulene. Lower: polycrystalline sample. Upper: calculated spectrum, Lorentzian full band width, 2Γ, equal to 5 cm^{-1}. Relative intensities on the vertical axis are scaled to make the strongest peaks match in appearance.

the case of **1**, each vibration is split into four components (A_1, A_2, B_1, B_2), all of them Raman and only three, except A_2, infrared active. Experimentally most infrared and Raman bands of both systems are single and not coincident. Exceptions, by comparison with solution spectra, are the infrared doublets 686/691, 753/760, 844/851, 1147/1151, and 1191/1195 cm^{-1} for **2** and 831/838 and 1245/1248 cm^{-1} for **1**. Possibly, the Raman peaks 193/198 cm^{-1} of **1** are a crystal doublet. The observed spectra are compared with calculations in Figures 6−9. The two sets of data match well on frequency and satisfactorily on intensity grounds. It may be seen that the infrared intensities of **1** and **2** are in very good agreement with solution data. Also the calculated Raman intensities (see Figures 7 and 9) compare fairly well with experiment, although the peaks below 400 cm^{-1} are weaker than observed. Therefore the calculated data may be taken as a guideline for the vibrational assignment.

The approximate classification of normal modes into bridge and ring vibrations is confirmed by our calculations. Modes with the largest amplitude along *x*, *y*, and *z* on the oxygen atom of **2** are calculated at 401, 993, and 868 cm^{-1}, respectively, and assigned as hindered oxygen translations B_1 (*x*), B_2 (*y*) and A_1 (*z*). These correspond to 402 (IR)/400 (R), 982 (IR), 862 (IR)/865 (R) cm^{-1} bands of **2** (see Figures 8 and 9). The equivalent modes of **1** are at 425, 933, and 878 cm^{-1} (419 (R), 931 (IR)/

934 (R), 874 (IR)/873(R) experimental values). Modes classified as hindered CH_2 rotations are calculated at 1011 (R_y, B_1), 1103 (R_z, A_2) and 1268 (R_x, B_2) cm^{-1} and observed at 1006 (IR), 1081 (R), and 1245, 1248 (IR) cm^{-1}. The CH_2 bending mode of A_1 symmetry occurs at 1475 cm^{-1} and is observed at 1447 (IR)/1453 (R) cm^{-1}. The calculated infrared and Raman intensities of these modes are in agreement with observations.

According to calculations, the strongest infrared and Raman bands of **1** and **2** are assigned to A_1 ring modes. These include the 755 (IR), 600 (R), and 318 (R) cm^{-1} peaks for **1** and the 753, 760 (IR), 623 (R), and 318 (R) cm^{-1} peaks for **2**. These vibrations are calculated at 762, 620, and 325 cm^{-1} (**1**) and at 753, 642, and 312 cm^{-1} (**2**). The A_1 butterfly motion is observed at 193, 198 (R, **1**) cm^{-1} and at 189 cm^{-1} (R, **2**) and calculated at 190 cm^{-1} (**1**) and 174 cm^{-1} (**2**).

The ring modes can be divided into three groups of bands, ≈150−500, ≈600−1000, and ≈1100−1650 cm^{-1}, as suggested experimentally and by the calculations. In the first interval eight modes are predicted. All of them are assigned in the spectrum of **2** and six in the spectrum of **1** (see Tables 3 and 4). In addition to the 307 cm^{-1} (B_1) mode, calculated weak in both the infrared and Raman spectra, the relatively intense Raman mode 175 cm^{-1} (A_2) is absent in the spectrum of **1**. In the second interval (≈600−1000 cm^{-1}) 16 vibrations must be considered according to calculations. Three (out of four) A_2 modes, 607, 963, and 870 cm^{-1} for **1** and 601, 958, and 796 cm^{-1} for **2**, are too weak to be observed in the Raman spectrum. One B_1 mode (939 cm^{-1}) of **1** and one B_1 (845 cm^{-1}) plus one B_2 (766 cm^{-1}) of **2**, predicted with small intensity in both spectra, are not observed. All others are easily assigned on the basis of frequency and intensity data (see again Tables 3 and 4). Finally, all 16 fundamentals of the third region have been identified on the spectra, except two **2** modes, 1266 and 1558 cm^{-1} of B_2 symmetry, and one, belonging to **1**, 1268 cm^{-1} of A_2 symmetry. The root-mean-square deviation, i.e., $[(1/n)\sum_1^n(\nu_{obs,i} - \nu_{calc,i})^2]^{1/2}$, of this assignment, not considering the C−H stretching vibrations, is ≈14 cm^{-1} for **1** and ≈13 cm^{-1} for **2**.

IV. Discussion

A correlation between the modes of naphthalene and the ring modes of **1** and **2** may be attempted on the basis of our DF results. With reference to the coordinate system of Figure 2, the correlation diagram $D_{2h} \rightarrow C_{2v}$ implies the following correspondence between symmetry species: (A_g, B_{1u}) → A_1, (B_{1g}, A_u) → A_2, (B_{2g}, B_{3u}) → B_1, (B_{3g}, B_{2u}) → B_2. Due to the loss of the molecular symmetry plane, the separation of naphthalene vibrations into in-plane (A_g, B_{1g}, B_{2u}, B_{3u}) and out-of-plane (B_{2g}, B_{3g}, A_u, B_{1u}) modes no longer holds for **1** and **2** and, as a consequence, all internal coordinates contribute in principle to each normal mode of bridged [10]annulenes. By careful inspection of their displacement vectors, it may be seen, however, that in most cases the overall character of the vibration is conserved on going from naphthalene to 1,6-bridged [10]-annulenes. Following these considerations the correspondence summarized in Table 5 is proposed. General comments are

1. The structural distortion of the decagon ring along *z* induces a π delocalization less extended in **1** and **2** than in naphthalene, thus weakening on the average diagonal and interaction force constants of the ring coordinates.

2. CH_2 and O bridges affect mainly vibrational modes with small or negligible displacements on the H atoms, i.e., C−C stretchings, CCC bendings, and CCCC out-of-plane torsions.

3. The largest frequency shift is found for modes localized on the C_1 and C_6 atoms of naphthalene.

TABLE 3: Observed Infrared (IR; cryst, Polycrystalline Film; sol, Solution) and Raman (R; Microcrystal) Frequencies (cm^{-1}) of 1,6-Methano[10]annulene (1) at Room Temperature; Calculated Frequencies (ω, cm^{-1}), Infrared and Raman Intensities (I_{ir} and I_R, Respectively, in Km mol^{-1} and Å^4 amu^{-1}); Mode Symmetry (sym) and Approximate Description;[a] DF/B3-LYP, 6-31G Calculation Using a Scale Factor 0.979 (See Text for Details)[b]**

IR			calcd				
cryst	sol	R	ω	I_{IR}	I_R	sym	
			175	0	6.3	A_2	τ_c
		{193 198	190	0.01	6.8	A_1	butterfly
			307	0.1	0.07	B_1	τ_c
		318	325	0.1	11.6	A_1	$C_1C_{11}C_6$bend, τ_H
		339	340	0.2	3.8	B_2	b_c
		368	370	0	3.6	A_2	b_c
		419	425	0.1	2.1	B_1	T_x
445		443	453	4.5	0.1	B_2	τ_c
474		473	481	4.2	6.1	A_1	b_c
		589	607	0	1.1	A_2	τ_c
599	602	600	620	23.9	49.6	A_1	$C_1C_{11}C_6$ bend, τ_H
642	642	642	633	0.5	1.8	B_2	τ_c
655	655		654	0.6	2.4	B_1	b_c
683	682	684	690	0.003	6.1	B_1	τ_H
751			761	1.4	1.7	B_2	b_c
755		760	762	66.0	15.7	A_1	τ_H
		792	793	0	0.02	A_2	τ_H
{831 838			842	19.6	2.6	B_2	τ_H
850		851	857	0.2	0.1	B_1	τ_H
			870	0	0.02	A_2	b_c
874	876	873	878	3.5	11.4	A_1	T_z
902		902	914	0.2	9.3	A_1	τ_H
931	932	934	933	2.7	4.7	B_2	T_y
			939	1.2	0.4	B_1	s_c, b_H
			963	0	0.08	A_2	τ_H
961	964	966	966	4.5	0.2	B_2	τ_H
		974	973	0.001	23.3	A_1	b_H, s_c
1006	1007		1011	4.9	0.5	B_1	R_y
		1081	1103	0	0.5	A_2	R_z
1127	1131	1128	1137	2.1	0.6	B_2	b_H
1163		1163	1174	0	15.5	A_2	b_H
1174	1176	1174	1189	5.1	0.1	B_1	b_H
		1200	1207	0.01	1.0	A_1	b_H
			1268	0	1.04	A_2	b_H
{1245 1248	1239		1268	4.9	0.6	B_2	R_x
		1261	1274	0.1	3.5	B_1	b_H
1305	1306		1316	0.5	0.09	B_2	b_H, s_c
1343	1345		1352	0.5	1.8	A_1	C_1-C_{11}, C_6-C_{11}
1355	1355	1356	1372	2.9	11.5	B_1	b_H, s_c
1398	1401		1410	2.5	0.0004	B_2	b_H, s_c
1431	1434	1432	1450	0.02	47.2	A_1	b_H, s_c
		1467	1471	0	11.9	A_2	b_H, s_c
1447	1448	1453	1475	8.3	6.6	A_1	CH_2 bend
1483	1485	1483	1510	1.9	27.3	A_1	s_c
1510	1514		1537	3.8	1.6	B_1	b_H, s_c
1533							
1544	1545		1561	3.0	1.9	B_2	s_c
		1645	1602	0	5.6	A_2	s_c

[a] s_c = C−C ring stretching; b_c = CCC ring bending; b_H = CCH ring bending; τ_H = out-of-plane CCCH bending; τ_c = CCCC torsion; T_x, T_y, T_z = hindered CH_2 translations; R_x, R_y, R_z = hindered CH_2 rotations (see text for details). [b] Frequency values in braces are crystal components of the molecular vibrations.

As a result, most in- and out-of-plane vibrations of naphthalene correlate with vibrations of **1** and **2** of lower frequency. However, in the case of the butterfly mode (173 cm^{-1}, naphthalene; 174 cm^{-1}, **2**; 190 cm^{-1}, **1**) the trend is reversed, suggesting a nonvanishing interaction of bridge atoms with the ring. Also for several in-plane modes, notably some B_{3u} modes, the change is opposite.

TABLE 4: Observed Infrared (IR; cryst, Polycrystalline Film; sol, Solution) and Raman (R; Microcrystal) Frequencies (cm^{-1}) of 1,6-Epoxy[10]annulene (2) at Room Temperature; Calculated Frequencies (ω, cm^{-1}), Infrared and Raman Intensities (I_{IR} and I_R, Respectively, in km mol^{-1} and $Å^4$ amu^{-1}); Mode Symmetry (sym) and Approximate Description;[a] DF/B3-LYP, 6-31G Calculation Using a Scale Factor 0.979 (See Text for Details)[b]**

IR			calcd				
cryst	sol	R	ω	I_{IR}	I_R	sym	
		176	145	0	5.6	A_2	τ_c
		189	174	1.2	3.7	A_1	butterfly
		309	325	0.02	0.5	B_1	τ_c
321		318	312	1.0	10.9	A_1	C_1OC_6bend, τ_H
352		351	349	1.1	1.9	B_2	τ_c
402		400	401	3.4	1.3	B_1	T_x
		411	412	0	5.5	A_2	b_c
450			455	2.1	0.3	B_2	τ_c
491		492	488	2.9	12.6	A_1	b_c
			601	0	1.5	A_2	τ_c
619	618	623	642	23.5	55.4	A_1	C_1OC_6bend, τ_H
637	633	641	657	0.1	1.6	B_2	τ_c
{686, 691}	683	687	687	0.2	5.9	B_1	τ_H
745			744	6.9	0.5	B_1	b_c
{753, 760}		760	753	62.3	12.6	A_1	τ_H
			766	0.1	0.8	B_2	b_c
		807	796	0	0.01	A_2	τ_H
{844, 851}		846	844	21.1	3.6	B_2	τ_H
			845	1.1	0.1	B_1	τ_H
862	867	865	868	24.0	9.7	A_1	T_z
885		883	880	0	0.3	A_2	b_c
		912	904	0.1	7.9	A_1	τ_H
			958	0	0.02	A_2	τ_H
946	946		961	0.9	0.3	B_2	τ_H
959	960	960	963	4.1	0.001	B_1	s_c, b_c
972	973	973	978	2.3	33.2	A_1	b_H, b_c
982	987		993	6.6	1.3	B_2	T_y
1115	1118	1116	1124	13.3	0.01	B_2	b_H
		1148	1142	0	5.2	A_2	b_H
{1147, 1151}	1148		1166	7.0	0.3	B_1	b_H
{1191, 1195}	1194	1193	1201	3.6	1.4	A_1	b_H
		1220	1227	0	10.9	A_2	b_H
1236	1239		1243	4.4	0.3	B_1	b_H
			1266	0.01	3.1	B_2	b_H
1319	1315	1319	1336	1.1	6.9	B_1	b_H, s_c
1326	1331		1341	12.8	2.1	A_1	C_1-C_6, C_6-C_{11}
1399	1398		1410	0.5	0.03	B_2	b_H
1441	1442	1442	1459	2.1	36.5	A_1	s_c, b_H
		1458	1471	0	20.5	A_2	s_c, b_H
1498		1497	1529	0.5	32.8	A_1	s_c
			1558	4.7	1.0	B_2	s_c
1535	1537		1564	16.0	0.3	B_1	s_c
		1634	1612	0	1.65	A_2	s_c

[a] s_c = C−C ring stretching; b_c = CCC ring bending; b_H = CCH ring bending; τ_H = out-of-plane CCCH bending; τ_c = CCCC torsion; T_x, T_y, T_z = hindered O translations (see text for details). [b] Frequency values in braces are crystal components of the molecular vibrations.

In the following we consider interesting points of our correlation table according to the symmetry species.

$$(A_g, B_{1u}) \rightarrow A_1$$

One B_{1u}, 482 cm^{-1}, and three A_g modes, 759, 1385, and 1594 cm^{-1}, have the largest displacements on the C_1, C_6 atom pair of naphthalene and are thus expected to be particularly sensitive to bridging. The two modes at lower frequency shift to 325 cm^{-1} (**1**), 312 cm^{-1} (**2**) and to 620 cm^{-1} (**1**), 642 cm^{-1} (**2**), strongly active in the Raman spectrum, assigned as symmetric and antisymmetric combinations of the methylenic (epoxide) bending with out-of-plane CCC−H ring bendings, respectively. The 1385 cm^{-1} C_1-C_6 stretching, the strongest peak in the Raman spectrum of naphthalene, is correlated with the symmetric (C_1, C_6)−O and (C_1, C_6)−C_{11} stretchings, 1341 and 1352 cm^{-1}, respectively, with much lower Raman intensity. The 1594 cm^{-1} mode, i.e., the simultaneous elongation of C_3-C_4, C_1-C_6 and C_8-C_9 bonds, is damped by the insertion of the bridge and corresponds in **1** and **2** to weakly interacting C_3-C_4 and C_8-C_9 stretchings, 1510 and 1529 cm^{-1}. The strongest infrared band of naphthalene, 786 cm^{-1}, assigned as out-of-plane H-bending of B_{1u} symmetry, and the relatively intense Raman peak, 509 cm^{-1}, the symmetric A_g CCC in-plane bending, do not involve C_1 and C_6 displacements. They shift less than previous modes, to 762 and 481 cm^{-1} in **1**, to 753 and 488 cm^{-1} in **2**, as expected. The 762 and 753 cm^{-1} modes are also the strongest in the infrared spectrum of **1** and **2**, respectively.

TABLE 5: Calculated Ring Frequencies (cm^{-1}; DF/B3-LYP Results, 6-31G Basis Set; 0.979 Scale Factor) of 1,6-Methano[10]annulene (1), 1,6-Epoxy[10]annulene (2), and Naphthalene (NA)[a]**

sym	**1**	**2**	NA		sym	**1**	**2**	NA	
A_1	481	488	509	A_g	A_2	370	412	507	B_{1g}
	620	642	759	A_g		870	880	928	B_{1g}
	973	978	1032	A_g		1174	1142	1153	B_{1g}
	1207	1201	1164	A_g		1268	1227	1246	B_{1g}
	1352	1341	1386	A_g		1471	1471	1470	B_{1g}
	1450	1459	1471	A_g		1602	1612	1651	B_{1g}
	1510	1529	1594	A_g					
	190	174	173	B_{1u}		175	145	186	A_u
	325	312	482	B_{1u}		607	601	620	A_u
	762	753	786	B_{1u}		793	796	836	A_u
	914	904	948	B_{1u}		963	958	969	A_u
B_1	654	744	622	B_{3u}	B_2	340	349	357	B_{2u}
	939	963	1021	B_{3u}		761	766	791	B_{2u}
	1189	1166	1153	B_{3u}		1137	1124	1130	B_{2u}
	1274	1243	1215	B_{3u}		1316	1266	1265	B_{2u}
	1372	1336	1378	B_{3u}		1410	1410	1395	B_{2u}
	1537	1564	1529	B_{3u}		1561	1558	1621	B_{2u}
	307	325	388	B_{2g}		453	455	471	B_{3g}
	690	687	720	B_{2g}		633	657	767	B_{3g}
	857	845	932	B_{2g}		842	844	880	B_{3g}
						966	961	976	B_{3g}

[a] The symmetry labels on the left refer to C_{2v} symmetry of **1** and **2** while those on the right refer to D_{2h} symmetry of NA, using the reference system of Figure 2.

$$(B_{2g}, B_{3u}) \rightarrow B_1$$

B_1 modes show weakly in the **1** and **2** spectra, in close agreement with the spectral behavior in naphthalene. Three B_{3u} modes, 622, 1215, 1529 cm^{-1}, for which the C_1 and C_6 atoms move along *x*, are correlated with modes of **1** and **2** of higher frequency. The vibrational analysis indicates that the *x* coordinate of these atoms is replaced by bending $C_2C_1C_{11}$ (or C_2C_1O). Out-of-plane B_{2g} modes, conserving substantially their out-of-plane character in **1** and **2**, shift appreciably to lower frequencies probably due to mass effect.

$$(B_{1g}, A_u) \rightarrow A_2; \quad (B_{3g}, B_{2u}) \rightarrow B_2$$

A_2 ring modes are inactive in the infrared and only weakly active in the Raman spectrum of **1** and **2**. Also the B_2 ring modes, though infrared and Raman active, do not contribute significantly to the spectra. The (B_{1g}, A_{1u}) → A_2 and (B_{3g}, B_{2u}) → B_2 correlations are good examples of the general behavior.

In fact, C_1 and C_6 displacements are found for the B_{1g} 507 and 1651 cm^{-1} modes, which are CCC bending and CC stretching, respectively, and for the B_{3g} 767 cm^{-1} mode, a CCCC out-of-plane torsion. Their frequency decreases on going to **1** and **2** (see Table 4). CCH bendings are much less influenced by bridging.

Finally, the excellent agreement between the solution and the calculated infrared spectrum of **2** (see Figure 8) should be emphasized. Since the DF calculation method correctly predicts the structures of **1** (aromatic annulene) and of its 11,11-dicyano derivative (norcaradiene tautomer), we feel confident that the absence of norcaradienic or polyolefinic minima in the S_0 energy surface of **2**, as it results from our DF calculations, is correct. The two points may be taken as a good indication, though not conclusive in view of the calculation deficiencies relative to the 11,11-dimethyl system, in favor of the C_{2v} symmetry for **2** in solution and of the nonoccurrence of a tautomeric equilibrium between forms **1** and **5**.

V. Conclusions

In this paper we have reported on the infrared and Raman spectra of 1,6-methano[10]annulene and 1,6-epoxy[10]annulene and presented a detailed vibrational analysis based on DF/B3-LYP calculations with the 6-31G** basis set.

The two major results of this study are

1. A complete assignment of their vibrational modes, conveniently classified as ring and bridge modes, is obtained. The correlation with naphthalene modes helps identify the ring modes more sensitive to bridging.

2. The aromatic form is the only stable structure of 1,6-epoxy and 1,6-methano[10]annulene in the ground state. The excellent agreement of the calculated with the solution spectrum supports the conclusion.

Since annulenic substructures occur in more complex geometries such as methano- and epoxyfullerene,[42−44] the present analysis may be useful to further investigate the vibrational properties of these systems[45] and their derivatives.

Acknowledgment. This work was supported by the Italian Consiglio Nazionale delle Ricerche (CNR) and Ministero dell'Università e della Ricerca Scientifica e Tecnologica (MURST).

References and Notes

(1) Garratt, P. *Aromaticity*; John Wiley and Sons: New York, 1986.
(2) Choi, C. H.; Kertesz, M. *J. Chem. Phys.* **1998**, *108*, 6681−6688.
(3) Masamune, S.; Hojo, K.; Hojo, K.; Bigam, G.; Rabenstein, D. L. *J. Am. Chem. Soc.* **1971**, *93*, 4966−4968.
(4) Vogel, E.; Roth, H. D. *Angew. Chem., Int. Ed. Engl.* **1964**, *3*, 228.
(5) Masamune, S.; Brooks, D. W. *Tetrahedron Lett.* **1977**, 3239−3240.
(6) Scott, L. T.; Brunsvold, W. R.; Kirms, M. A.; Erden, I. *Angew. Chem., Int. Ed. Engl.* **1981**, *20*, 274.
(7) Scott, L. T.; Brunsvold, W. R.; Kirms, M. A.; Erden, I. *J. Am. Chem. Soc.* **1981**, *103*, 5216−5220.
(8) Masamune, S.; Brooks, D. W.; Morio, K.; Sobezak, R. L. *J. Am. Chem. Soc.* **1976**, *98*, 8277−8279.
(9) Gilchrist, T. L.; Tuddenham, D.; McCague, R.; Moody, C. D.; Rees, C. W. *J. Chem. Soc., Chem. Commun.* **1981**, 657−658.
(10) McCague, R.; Moody, C. D.; Rees, C. W. *J. Chem. Soc., Chem. Commun.* **1982**, 497−499.
(11) Meyers, A. G.; Finney, N. S. *J. Am. Chem. Soc.* **1992**, *114*, 10986−10987.
(12) Bianchi, R.; Pilati, T.; Simonetta, M. *Acta Crystallogr.* **1980**, *B36*, 3146−3148.
(13) Bianchi, R.; Morosi, G.; Mugnoli, A.; Simonetta, M. *Acta Crystallogr.* **1973**, *B29*, 1196−1208.
(14) Bianchi, R.; Pilati, T.; Simonetta, M. *Acta Crystallogr.* **1978**, *B34*, 2157−2162.
(15) Vogel, E.; Scholl, T.; Lex, J.; Hohlneicher, G. *Angew. Chem., Int. Ed. Engl.* **1982**, *21*, 869−870.
(16) Neidlein, R.; Wirth, W.; Gieren, A.; Lamm, V.; Hubner, T. *Angew. Chem., Int. Ed. Engl.* **1985**, *24*, 587.
(17) Bailey, N. A.; Mason, R. *Chem. Commun.* **1967**, 1039−1040.
(18) Vogel, E. *Pure Appl. Chem.* **1982**, *54*, 1015−1039.
(19) Briat, B.; Schooley, D. A.; Records, R.; Bunnenberg, E.; Djerassi, C.; Vogel, E. *J. Am. Chem. Soc.* **1968**, *90*, 4691−4697.
(20) Klingensmith, K. A.; Puttmann, W.; Vogel, E.; Michl, J. *J. Am. Chem. Soc.* **1983**, *105*, 3375−3380.
(21) Dewey, H. J.; Deger, H.; Frolich, W.; Dick, B.; Klingensmith, K. A.; Hohlneicher, G.; Vogel, E.; Michl, J. *J. Am. Chem. Soc.* **1980**, *102*, 6412−6417.
(22) Dorn, H. C.; Yannoni, C. S.; Lumbach, H.-H.; Vogel, E. *J. Phys. Chem.* **1994**, *98*, 11628−11629.
(23) Catani, L.; Gellini, C.; Salvi, P. R.; Marconi, G. *J. Photochem. Photobiol. A* **1997**, *105*, 123−127.
(24) Catani, L.; Gellini, C.; Salvi, P. R. *J. Phys. Chem. A* **1998**, *102*, 1945−1953.
(25) Bell, S.; Crayston, J. A.; Dines, T. J.; Ellahi, S. B. *J. Phys. Chem.* **1996**, *100*, 5252−5260.
(26) Sabljic, A.; Trinajstic, N. *J. Org. Chem.* **1981**, *46*, 3457−3461.
(27) Farnell, L.; Kao, J.; Radom, L.; Schaefer, H. F., III *J. Am. Chem. Soc.* **1981**, *103*, 2147−2151.
(28) Farnell, L.; Radom, L. *J. Am. Chem. Soc.* **1982**, *104*, 7650−7654.
(29) Cremer, D.; Dick, B. *Angew. Chem., Int. Ed. Engl.* **1982**, *21*, 865−866.
(30) Haddon, R. C.; Raghavachari, K. *J. Am. Chem. Soc.* **1985**, *107*, 289−298.
(31) Sironi, M.; Raimondi, M.; Cooper, D. L.; Gerratt, J. *J. Mol. Struct. (THEOCHEM)* **1995**, *338*, 257−265.
(32) Espinosa-Muller, A.; Meezes, F. C. *J. Chem. Phys.* **1978**, *69*, 367−372.
(33) Becke, A. D. *Phys. Rev. A* **1988**, *33*, 3098−3100.
(34) Lee, C.; Yang, W.; Parr, R. G. *Phys. Rev. B* **1988**, *37*, 785−789.
(35) Frisch, M. J.; Trucks, G. W.; Schlegel, H. B.; Scuseria, G. E.; Gill, P. M. W.; Stratmann, R. E.; Burant, J. C.; Dapprich, S.; Millam, J. M.; Daniels, A. D.; Kudin, K. N.; Strain, M. C.; Farkas, O.; Tomasi, J.; Barone, V.; Cossi, M.; Cammi, R.; Mennucci, B.; Pomelli, C.; Adamo, C.; Clifford, S.; Ochterski, J.; Johnson, B. G.; Robb, M. A.; Cheeseman, J. R.; Keith, T.; Petersson, G. A.; Montgomery, J. A.; Raghavachari, K.; Al-Laham, M. A.; Zakrzewski, V. G.; Ortiz, J. V.; Foresman, J. B.; Cioslowski, J.; Stefanov, B. B.; Liu, G.; Liashenko, A.; Piskorz, P.; Komaromi, I.; Cui, Q.; Morokuma, K.; Nanayakkara, A.; Challacombe, M.; Malik, D. K.; Rabuk, A. D.; Peng, C. Y.; Ayala, P. Y.; Chen, W.; Wong, M. W.; Andres, J. L.; Replogle, E. S.; Gomperts, R.; Martin, R. L.; Fox, D. J.; Binkley, J. S.; Defrees, D. J.; Baker, J.; Stewart, J. P.; Head-Gordon, M.; Gonzalez, C.; Pople, J. A. *Gaussian 98, Revision A.1;* Gaussian Inc.: Pittsburgh, PA, 1998.
(36) Brock, C. P.; Dunitz, J. D. *Acta Crystallogr.* **1982**, *B38*, 2218−2228.
(37) Schweig, A.; Thiel, W. *J. Am. Chem. Soc.* **1981**, *103*, 1420−1425.
(38) Jug, K.; Fasold, E. *J. Am. Chem. Soc.* **1987**, *109*, 2263−2265.
(39) Yoshizawa, K.; Kato, T.; Yamabe, T. *J. Phys. Chem.* **1996**, *100*, 5697−5701.
(40) Rauhut, G.; Pulay, P. *J. Phys. Chem.* **1995**, *99*, 3093−3100.
(41) Scott, A. P.; Radom, L. *J. Phys. Chem.* **1996**, *100*, 16502−16513.
(42) Suzuki, T.; Li, Q.; Khemani, K. C.; Wudl, F. *J. Am. Chem. Soc.* **1992**, *114*, 7301−7302.
(43) Smith, A. B., III; Strongin, R. M.; Brard, L.; Furst, G. T.; Romanow, W. J.; Owens, K. G.; King, R. C. *J. Am. Chem. Soc.* **1993**, *115*, 5829−5830.
(44) Creegan, K. M.; Robbins, J. L.; Robbins, W. K.; Millar, J. M.; Sherwood, R. D.; Tindall, P. J.; Cox, D. M.; Smith, A. B., III; McCauley, J. P., Jr.; Jones, D. R.; Gallagher, R. T. *J. Am. Chem. Soc.* **1992**, *114*, 1103−1105.
(45) Cardini, G.; Bini, R.; Salvi, P. R.; Schettino, V.; Klein, M. L.; Strongin, R. M.; Brard, L.; Smith, A. B., III *J. Phys. Chem.* **1994**, *98*, 9966−9971.